New arsenate minerals from the Arsenatnaya fumarole, Tolbachik volcano, Kamchatka, Russia. XX. Evseevite, $Na_2Mg(AsO_4)F$, the first natural arsenate with antiperovskite structure

Igor V. Pekov[1]*, Natalia V. Zubkova[1], Atali A. Agakhanov[2], Marina F. Vigasina[1], Vasiliy O. Yapaskurt[1], Sergey N. Britvin[3], Anna G. Turchkova[1], Evgeny G. Sidorov[4†], Elena S. Zhitova[4] and Dmitry Yu. Pushcharovsky[1]

[1]Faculty of Geology, Moscow State University, Vorobievy Gory, 119991 Moscow, Russia

[2]Fersman Mineralogical Museum of the Russian Academy of Sciences, Leninsky Prospekt 18-2, 119071 Moscow, Russia

[3]Dept. of Crystallography, St Petersburg State University, University Embankment 7/9, 199034 St Petersburg, Russia

[4]Institute of Volcanology and Seismology, Far Eastern Branch of Russian Academy of Sciences, Piip Boulevard 9, 683006 Petropavlovsk-Kamchatsky, Russia

*E-mail: igorpekov@mail.ru

† Deceased 20 March 2021

Running title: Evseevite, a new mineral

Prepublished Article

Abstract

The new mineral evseevite was found in the Arsenatnaya fumarole, Second scoria cone of the Northern Breakthrough of the Great Tolbachik Fissure Eruption, Tolbachik volcano, Kamchatka, Russia. Evseevite is represented by two chemical varieties. The variety close to the end-member $Na_2Mg(AsO_4)F$ (holotype) is associated with sanidine, hematite, tenorite, aegirine, cassiterite, sylvite, halite, johillerite, badalovite, calciojohillerite, hatertite, arsmirandite, yurmarinite, axelite, polyarsite, aphthitalite, potassic-magnesio-fluoro-arfvedsonite, litidionite, ferrisanidine,

This is a 'preproof' accepted article for Mineralogical Magazine. This version may be subject to change during the production process.
DOI: 10.1180/mgm.2023.50

https://doi.org/10.1180/mgm.2023.50 Published online by Cambridge University Press

and tridymite. The P- and S-enriched variety (cotype) is associated with hematite, fluorophlogopite, svabite, fluorapatite, tilasite, calciojohillerite, forsterite, cassiterite, belomarinaite, and aphthitalite. Evseevite occurs as prismatic, acicular or hair-like crystals up to 0.7 mm long combined in clusters up to 0.5 mm, brushes or crusts up to 2 × 2 mm. It is transparent, colourless or pale pinkish, with vitreous lustre. D_{calc} is 3.377 g cm^{-3} for holotype and 3.226 g cm^{-3} for cotype. Evseevite is optically uniaxial (+), α 1.545(2), β 1.546(2), γ 1.549(2), and $2V_{meas}$ 40(10)°. The empirical formulae calculated based on O+F = 5 *apfu* are $(Na_{1.99}Ca_{0.03}K_{0.01})_{\Sigma 2.03}(Mg_{0.98}Fe^{3+}_{0.01}Zn_{0.01}Cu_{0.01})_{\Sigma 1.01}[(As_{0.98}Si_{0.01})_{\Sigma 1.01}O_4](F_{0.97}O_{0.03})$ for holotype and $Na_{2.02}(Mg_{1.00}Fe^{3+}_{0.03})_{\Sigma 1.03}[(As_{0.69}P_{0.25}S_{0.07})_{\Sigma 1.01}O_4](F_{0.78}O_{0.22})$ for cotype. Evseevite is orthorhombic, *Pbcn*, *a* 5.3224(1), *b* 14.1255(3), *c* 12.0047(3) Å, *V* 902.53(4) Å^3 and *Z* = 8. Strong reflections of the powder XRD pattern [*d*,Å(*I*)(*hkl*)] are: 4.001(100)(121), 3.479(56)(023), 3.041(45)(042), 2.657(44)(200), 2.642(68)(142) and 2.613(36)(104). The crystal structure was solved from single-crystal XRD data and refined on powder data by Rietveld method, R_{wp} = 0.0068, R_p = 0.0047, R_{obs} = 0.0435. Evseevite is isostructural to moraskoite $Na_2Mg(PO_4)F$. The structure of evseevite can be described in terms of anion-centred polyhedra. F-centred octahedra $[FNa_4Mg_2]^{7+}$ share faces to form chains $[FNa_2Mg]^{3+}$ and AsO_4 tetrahedra are located between the chains. Evseevite belongs to quite few minerals with antiperovskite structures being the first natural arsenate with antiperovskite units. The mineral is named in honor of the Russian mineralogist Aleksandr Andreevich Evseev (born 1949).

Keywords: evseevite; new mineral; sodium magnesium fluorarsenate; crystal structure; anion-centred octahedron; antiperovskite structure; fumarole sublimate; Tolbachik volcano.

Prepublished Article

Introduction

This paper continues the series of articles in which we characterize new arsenates from the Arsenatnaya fumarole at the Second scoria cone of the Northern Breakthrough of the Great Tolbachik Fissure Eruption 1975–1976 (NB GTFE), Tolbachik volcano, Kamchatka Peninsula, Far-Eastern Region, Russia. Twenty two new mineral species were described in the previous papers of the series: yurmarinite $Na_7(Fe^{3+},Mg,Cu)_4(AsO_4)_6$ (Pekov *et al*., 2014a), two polymorphs of $Cu_4O(AsO_4)_2$, ericlaxmanite and kozyrevskite (Pekov *et al*., 2014b), popovite $Cu_5O_2(AsO_4)_2$ (Pekov *et al*., 2015a), structurally related shchurovskyite $K_2CaCu_6O_2(AsO_4)_4$ and dmisokolovite $K_3Cu_5AlO_2(AsO_4)_4$ (Pekov *et al*., 2015b), katiarsite $KTiO(AsO_4)$ (Pekov *et al*., 2016a), melanarsite $K_3Cu_7Fe^{3+}O_4(AsO_4)_4$ (Pekov *et al*., 2016b), pharmazincite $KZnAsO_4$ (Pekov *et al*., 2017), arsenowagnerite $Mg_2(AsO_4)F$ (Pekov *et al*., 2018b), arsenatrotitanite $NaTiO(AsO_4)$ (Pekov *et al*., 2019a), the two isostructural minerals edtollite $K_2NaCu_5Fe^{3+}O_2(AsO_4)_4$ and

https://doi.org/10.1180/mgm.2023.50 Published online by Cambridge University Press

alumoedtollite $K_2NaCu_5AlO_2(AsO_4)_4$ (Pekov *et al*., 2019b), anatolyite $Na_6(Ca,Na)(Mg,Fe^{3+})_3Al(AsO_4)_6$ (Pekov *et al*., 2019c), zubkovaite $Ca_3Cu_3(AsO_4)_4$ (Pekov *et al*., 2019d), pansnerite $K_3Na_3Fe^{3+}_6(AsO_4)_8$ (Pekov *et al*., 2020a), badalovite $NaNaMg(MgFe^{3+})(AsO_4)_3$ (Pekov *et al*., 2020b), calciojohillerite $NaCaMgMg_2(AsO_4)_3$ (Pekov *et al*., 2021a), yurgensonite $K_2SnTiO_2(AsO_4)_2$ (Pekov *et al*., 2021b), paraberzeliite $NaCaCaMg_2(AsO_4)_3$ (Pekov *et al*., 2022a), khrenovite $Na_3Fe^{3+}_2(AsO_4)_3$ (Pekov *et al*., 2022b), and axelite $Na_{14}Cu_7(AsO_4)_8F_2Cl_2$ (Pekov *et al*., 2023).

In this article we describe the new mineral evseevite (Cyrillic: евсеевит), ideally $Na_2Mg(AsO_4)F$. It is named in honour of the Russian mineralogist Aleksandr Andreevich Evseev (born 1949) who works in Fersman Mineralogical Museum of the Russian Academy of Sciences, Moscow. He is a specialist in history of mineralogy and an application of geographical information in mineralogy.

Both the new mineral and its name have been approved by the IMA Commission on New Minerals, Nomenclature and Classification (IMA CNMNC), IMA2019–064. The holotype specimen is deposited in the systematic collection of the Fersman Mineralogical Museum, Moscow with the catalogue number 96701.

Preprinted Article

Occurrence and general appearance

The Arsenatnaya fumarole, discovered by us in 2012, is located at the summit of the Second scoria cone of the NB GTFE, a monogenetic volcano formed in 1975 (Fedotov and Markhinin, 1983). Arsenatnaya is one of the hottest Tolbachik fumaroles today: the temperatures measured by us using a chromel-alumel thermocouple in the period 2012–2022, reach 500°C in its deep levels. It is a locality greatly outstanding in mineral diversity and originality: more than 200 mineral species have been reliably identified here, including 67 new minerals. The mineralogy and zonation of sublimate incrustations of Arsenatnaya were recently described by Pekov *et al*. (2018a) and Shchipalkina *et al*. (2020); the general mineralogical features of oxidizing-type fumaroles of Tolbachik were overviewed by Vergasova and Filatov (2016) and Pekov *et al*. (2020c).

The specimens with the new mineral were first collected by us in July 2018 from hot pockets situated 1.5–2 m below the day surface, within the zone IV (Shchipalkina *et al*., 2020), or polymineralic zone. Evseevite is represented by two chemical varieties. The variety close to the end-member $Na_2Mg(AsO_4)F$ gave the specimen considered as the holotype (sample #6328[1]): all complex of studies was carried out for this variety, including the crystal structure determination.

[1] ##6328, 6260 and 7529 are authors' working numbers of the three studied samples; #6328 is corresponding to the catalogue number 96701 in the systematic collection of the Fersman Mineralogical Museum (see Introduction).

https://doi.org/10.1180/mgm.2023.50 Published online by Cambridge University Press

The variety enriched with admixed P and S, which partially substitute As, is considered as the cotype (#6260): scanning electron microscopy (SEM), electron microprobe analysis (EMPA) and powder X-ray diffraction (XRD) study were performed for this variety. Additional specimens of the variety chemically close to the holotype but morphologically different were collected from other pockets in the same area in July 2022 (#7529). The temperature measured in the pockets with evseevite during sampling varied from 380 to 450°C.

These chemical varieties of evseevite occur in different mineral assemblages. In holotype and later collected specimen #7529, the new mineral is associated with sanidine, hematite, tenorite, aegirine, cassiterite, sylvite, halite, johillerite, badalovite, calciojohillerite, hatertite, arsmirandite, yurmarinite, axelite, polyarsite, aphthitalite, potassic-magnesio-fluoro-arfvedsonite, litidionite, ferrisanidine, and tridymite. In the cotype specimen, evseevite is associated with hematite, fluorophlogopite, svabite, fluorapatite, tilasite, calciojohillerite, forsterite, cassiterite, belomarinaite, and aphthitalite.

Evseevite occurs in cavities as prismatic, typically long-prismatic to acicular or hair-like crystals up to 0.1 mm, rarely up to 0.7 mm long and up to 0.03 mm thick. They are elongated along [100] and usually combined in parallel, near-parallel, sheaf-, bush- or brush-like aggregates. Clusters (up to 0.5 mm across) of randomly oriented crystals are also common. Acicular crystals form interrupted brushes and hair-like crystals compose pilous crusts (Fig. 1) up to 2 × 2 mm in area. Some crystals are skeletal, case-like.

We suggest that evseevite was deposited directly from the gas phase as a volcanic sublimate or, more probably, formed as a result of the interaction between fumarolic gas and basalt scoria at the temperatures not lower than 450ºC. Basalt could be a source of Mg which has low volatility in such fumarolic systems (Symonds and Reed, 1993).

Preprinted Article

Physical properties and optical data

Evseevite is transparent, colourless or pale pinkish, with white streak and vitreous lustre. The mineral is brittle, cleavage or parting was not observed. The fracture is uneven. Density calculated using the empirical formula and unit-cell volume found from powder XRD data is 3.377 g cm^{-3} for the holotype and 3.226 g cm^{-3} for the P- and S-enriched cotype.

The optical data were obtained for the holotype specimen. It is optically biaxial (+), α = 1.545(2), β = 1.546(2), γ = 1.549(2), $2V_{meas}$ = 40(10)° and $2V_{calc}$ = 60° (589 nm). Dispersion of optical axes was not observed. Orientation: $X = a$. Extinction is straight and elongation is negative. In transmitted plane-polarized light the mineral is colourless and non-pleochroic.

Raman Spectroscopy

https://doi.org/10.1180/mgm.2023.50 Published online by Cambridge University Press

The Raman spectrum of the holotype evseevite (Fig. 2) was obtained on a randomly oriented crystal using an EnSpectr R532 instrument with a green laser (532 nm) at room temperature. The output power of the laser beam was about 10 mW. The spectrum was processed using the EnSpectr expert mode program in the range from 4000 to 100 cm^{-1} with the use of a holographic diffraction grating with 1800 lines per cm^{-1} and a resolution of 6 cm^{-1}. The diameter of the focal spot on the sample was about 10 μm. The backscattered Raman signal was collected with a 40x objective; signal acquisition time for a single scan of the spectral range was 1500 ms and the signal was averaged over 20 scans.

The bands in the Raman spectrum of evseevite are assigned according to Nakamoto (1986). Bands in the region between 950 and 770 cm^{-1} correspond to As^{5+}–O stretching vibrations of AsO_4^{3-} anions. The presence of two strong bands in this region (with maxima at 883 and 808 cm^{-1}) is caused by significant distortion of AsO_4 tetrahedron (see below). Bands with frequencies lower than 520 cm^{-1} correspond to bending vibrations of AsO_4 tetrahedra, Mg–O stretching vibrations and lattice modes. The absence of bands with frequencies higher than 950 cm^{-1} indicates the absence of groups with O–H, C–H, C–O, N–H, N–O and B–O bonds in evseevite.

Chemical composition

The chemical composition of evseevite was studied by EMPA using a Jeol JSM-6480LV scanning electron microscope equipped with an INCA-Wave 500 wavelength-dispersive spectrometer (Laboratory of Analytical Techniques of High Spatial Resolution, Dept. of Petrology, Moscow State University), with an acceleration voltage of 20 kV, a beam current of 20 nA, and a 3 μm beam diameter.

The chemical data in wt% are given in Table 1. Contents of other elements with atomic numbers higher than carbon were below detection limits.

The empirical formulae calculated on the basis of O+F = 5 atoms per formula unit are $(Na_{1.99}Ca_{0.03}K_{0.01})_{\Sigma 2.03}(Mg_{0.98}Fe^{3+}_{0.01}Zn_{0.01}Cu_{0.01})_{\Sigma 1.01}[(As_{0.98}Si_{0.01})_{\Sigma 1.01}O_4](F_{0.97}O_{0.03})$ for holotype and $Na_{2.02}(Mg_{1.00}Fe^{3+}_{0.03})_{\Sigma 1.03}[(As_{0.69}P_{0.25}S_{0.07})_{\Sigma 1.01}O_4](F_{0.78}O_{0.22})$ for cotype. The idealised formula is $Na_2Mg(AsO_4)F$ which requires Na_2O 27.16, MgO 17.66, As_2O_5 50.36, F 8.33, –O=F –3.51, total 100 wt%.

The Gladstone–Dale compatibility index (Mandarino, 1981) for the holotype evseevite, $1 - (K_p/K_c) = 0.028$, excellent.

X-ray crystallography and crystal structure determination details

Pre-Published Article

https://doi.org/10.1180/mgm.2023.50 Published online by Cambridge University Press

Single-crystal XRD studies of the holotype sample of evseevite were carried out at room temperature using an Xcalibur S diffractometer equipped with a CCD detector (Mo*K*α-radiation). Powder XRD data for both holotype and cotype samples were collected with a Rigaku R-AXIS Rapid II single-crystal diffractometer equipped with cylindrical image plate detector (radius 127.4 mm) using Debye-Scherrer geometry, Co*K*α radiation (rotating anode with VariMAX microfocus optics), 40 kV, 15 mA, and exposure 15 min. Angular resolution of the detector is 0.045 2Θ (pixel size 0.1 mm). The data were integrated using the software package Osc2Tab (Britvin *et al*., 2017). Powder XRD data (in Å for Co*K*α) for the holotype are given in Table 2. The strongest reflections of powder XRD patterns and unit-cell parameters calculated from powder data for both holotype and cotype are presented in Table 3.

The single-crystal XRD dataset used for the structure model determination was obtained on the same diffractometer Xcalibur S CCD. Data reduction was performed using CrysAlisPro, version 1.171.37.34 (Agilent..., 2014). The data were corrected for Lorentz factor and polarization effects. The crystal structure was solved by direct methods and refined in the space group *Pbcn* using the SHELX software package (Sheldrick, 2015). Low quality of the crystal and consequently of the experimental data precluded excellent agreement between observed and calculated *F* values but resulted in acceptable agreement with R_{hkl} = 0.1106 for 1116 reflections with $I>2\sigma(I)$. Reasonable values of interatomic distances and displacement parameters of atoms, as well as good agreement between the measured and calculated powder XRD patterns (Table 2; Fig. 3) showed that the obtained structure model is correct. Further refinement of the structure of holotype evseevite was performed by Rietveld method using this model.

Data treatment and the Rietveld structure analysis were carried out using JANA2006 program package (Petříček *et al*., 2006). The profiles were modeled using a pseudo-Voigt function. The structure was refined in isotropic approximation of atomic thermal displacements, the values of U_{iso} for all anions were restricted to be equal. The interatomic distances for As-centred tetrahedron and Mg-centred octahedron were softly restrained nearby the values obtained for the single-crystal model. Final agreement factors are: R_{wp} = 0.0068, R_p = 0.0047, R_{obs} = 0.0435. The observed and calculated powder XRD diagrams demonstrate very good agreement (Fig. 3; Table 2).

Data collection information and structure refinement details for both single-crystal and powder XRD studies are presented in Table 4, coordinates and thermal displacement parameters of atoms are given in Table 5, selected interatomic distances in Table 6, and bond valence calculations in Table 7. The data presented in Tables 5–7 are obtained in the result of the Rietveld refinement.

Preprinted Article

https://doi.org/10.1180/mgm.2023.50 Published online by Cambridge University Press

Discussion

Evseevite, ideally $Na_2Mg(AsO_4)F$, is the isostructural arsenate analogue of moraskoite $Na_2Mg(PO_4)F$ (Karwowski *et al*., 2015) and synthetic $Na_2Mg(PO_4)F$ (Swafford and Holt, 2002). The structure of evseevite (Fig. 4a) is based upon the heteropolyhedral (010) layers formed by [100] chains of Mg-centred octahedra connected *via* AsO_4 tetrahedra (Fig. 4b). A repeat unit of the chain is dimer $[Mg_2O_6F_2]^{10-}$ consisting of two MgO_4F_2 octahedra sharing common face O(2)–F(1)–O(2). Adjacent dimers are linked *via* F(2) vertices. Na cations occupy two crystallographically non-equivalent sites. Na(1) cations centre $Na(1)O_4F_2$ octahedra [in moraskoite this site centres seven-fold polyhedron with one elongated Na(1)–O(1) distance of 2.93 Å; in evseevite this distance is more than 3.0 Å and, thus, O(1) is excluded from the coordination sphere of Na(1) cation]. Na(2) cations occupy seven-fold polyhedra $Na(2)O_5F_2$. The Na(1) sites are located between the heteropolyhedral layers whereas the Na(2) sites are situated at both sides of the heteropolyhedral layer.

The crystal structure of evseevite, as well as of moraskoite, can be described in terms of anion-centred polyhedra. Both F(1) and F(2) sites are octahedrally coordinated by two Mg and four Na cations each. F-centred octahedra $[FNa_4Mg_2]^{7+}$ share faces to form [100] chains $[FNa_2Mg]^{3+}$; AsO_4 tetrahedra are located between the chains (Fig. 5). This approach was used for the description of nacaphite $Na_2Ca(PO_4)F$ (Krivovichev *et al*., 2007), the monoclinic ($P2_1/c$) mineral which is structurally related to moraskoite and evseevite and has the same stoichiometry. The relation of the crystal structures and unit-cell metrics of nacaphite and moraskoite were in detail reported by Karwowski *et al*. (2015).

Evseevite, moraskoite and nacaphite belong to quite few minerals with antiperovskite structure, *i.e*., have perovskite-type structures but with anions replaced by cations and *vice versa*. Earlier known natural antiperovskites include sulfates, phosphates and silicates (Krivovichev, 2008; Karwowski *et al*., 2015). Evseevite is the first arsenate mineral with antiperovskite units: its structure is based on F-centred octahedra $[FNa_4Mg_2]^{7+}$ which form chains similar to those in hexagonal 2*H*-perovskites. We have not found an information on synthetic arsenate antiperovskites in literature and databases, however, the *X*-centred octahedra $[XNa_6]^{5+}$ (*X* = F, OH) are present in the structures of synthetic cubic arsenates $Na_7F(AsO_4)_2\cdot 19H_2O$ and $Na_7(OH)(AsO_4)_2\cdot 19H_2O$ (Baur and Tillmanns, 1974) isostructural to the mineral natrophosphate, ideally $Na_7F(PO_4)_2\cdot 19H_2O$. Avdontceva *et al*. (2021) suggested that the presence of the $[FNa_6]^{5+}$ units makes it possible to consider natrophosphate-type compounds as a precursor for the formation of antiperovskite structure motifs based upon anion-centred octahedra.

Acknowledgements

Preprinted Article

https://doi.org/10.1180/mgm.2023.50 Published online by Cambridge University Press

We are grateful to Dmitry I. Belakovskiy and Margarita S. Avdontceva for their help. We also thank Oleg I. Siidra and anonymous referee for valuable comments. The mineralogical, spectroscopic and crystal chemical studies of evseevite by IVP, NVZ, MFV and DYP were supported by the Russian Science Foundation, grant no. 19-17-00050. The technical support by the SPbSU X-Ray Diffraction Resource Center in the powder XRD study is acknowledged.

References

Agilent Technologies, (2014) CrysAlisPro Software system, version 1.171.37.34, Agilent Technologies UK Ltd, Oxford, UK.

Avdontceva M., Krivovichev S. and Yakovenchuk V. (2021) Natrophosphate, Arctic mineral and nuclear waste phase: Structure refinements and chemical variability. *Minerals*, **11**, paper 186.

Baur W.H. and Tillmanns E. (1974) Salt hydrates. X. The crystal structure determinations of heptasodium fluoride bisphosphate 19-hydrate and heptasodium fluoride bisarsenate 19-hydrate and the computer simulation of the isomorphous vanadate salt. *Acta Crystallographica*, **B30**, 2218–2224.

Brese N.E. and O'Keeffe N.E. (1991) Bond-valence parameters for solids. *Acta Crystallographica*, **47**, 192–197.

Britvin S.N., Dolivo-Dobrovolsky D.V. and Krzhizhanovskaya M.G. (2017) Software for processing the X-ray powder diffraction data obtained from the curved image plate detector of Rigaku RAXIS Rapid II diffractometer. *Zapiski Rossiiskogo Mineralogicheskogo Obshchestva*, **146**, 104–107 (in Russian).

Fedotov S.A. and Markhinin Y.K., eds. (1983) *The Great Tolbachik Fissure Eruption*. Cambridge University Press, New York, 341 pp.

Gagné O.C. and Hawthorne F.C. (2015) Comprehensive derivation of bond-valence parameters for ion pairs involving oxygen. *Acta Crystallographica*, B**71**, 562–578.

Karwowski Ł., Kusz J., Muszyński A., Kryza R., Sitarz M. and Galuskin, E.V. (2015) Moraskoite, $Na_2Mg(PO_4)F$, a new mineral from the Morasko IAB-MG iron meteorite (Poland). *Mineralogical Magazine*, **79**, 387–398.

Krivovichev S.V. (2008) Minerals with antiperovskite structure: a review. *Zeitschrift für Kristallographie*, **223**, 109–113.

Krivovichev S.V., Yakovenchuk V.N., Ivanyuk G.Y., Pakhomovsky Y.A., Armbruster T. and Selivanova E.A. (2007) The crystal structure of nacaphite, $Na_2Ca(PO_4)F$: a re-investigation. *Canadian Mineralogist*, **45**, 915–920.

Preprinted Article

https://doi.org/10.1180/mgm.2023.50 Published online by Cambridge University Press

Mandarino J.A. (1981) The Gladstone-Dale relationship. Part IV. The compatibility concept and its application. *Canadian Mineralogist*, **14**, 498–502.

Nakamoto K. (1986) *Infrared and Raman Spectra of Inorganic and Coordination Compounds*. John Wiley & Sons, New York.

Pekov I.V., Zubkova N.V., Yapaskurt V.O., Belakovskiy D.I., Lykova I.S., Vigasina M.F., Sidorov E.G. and Pushcharovsky D.Yu. (2014a) New arsenate minerals from the Arsenatnaya fumarole, Tolbachik volcano, Kamchatka, Russia. I. Yurmarinite, $Na_7(Fe^{3+},Mg,Cu)_4(AsO_4)_6$. *Mineralogical Magazine*, **78**, 905–917.

Pekov I.V., Zubkova N.V., Yapaskurt V.O., Belakovskiy D.I., Vigasina M.F., Sidorov E.G. and Pushcharovsky D.Yu. (2014b) New arsenate minerals from the Arsenatnaya fumarole, Tolbachik volcano, Kamchatka, Russia. II. Ericlaxmanite and kozyrevskite, two natural modifications of $Cu_4O(AsO_4)_2$. *Mineralogical Magazine*, **78**, 1527–1543.

Pekov I.V., Zubkova N.V., Yapaskurt V.O., Belakovskiy D.I., Vigasina M.F., Sidorov E.G. and Pushcharovsky D.Yu. (2015a) New arsenate minerals from the Arsenatnaya fumarole, Tolbachik volcano, Kamchatka, Russia. III. Popovite, $Cu_5O_2(AsO_4)_2$. *Mineralogical Magazine*, **79**, 133–143.

Pekov I.V., Zubkova N.V., Belakovskiy D.I., Yapaskurt V.O., Vigasina M.F., Sidorov E.G. and Pushcharovsky D.Yu. (2015b) New arsenate minerals from the Arsenatnaya fumarole, Tolbachik volcano, Kamchatka, Russia. IV. Shchurovskyite, $K_2CaCu_6O_2(AsO_4)_4$, and dmisokolovite, $K_3Cu_5AlO_2(AsO_4)_4$. *Mineralogical Magazine*, **79**, 1737–1753.

Pekov I.V., Yapaskurt V.O., Britvin S.N., Zubkova N.V., Vigasina M.F. and Sidorov E.G. (2016a) New arsenate minerals from the Arsenatnaya fumarole, Tolbachik volcano, Kamchatka, Russia. V. Katiarsite, $KTiO(AsO_4)$. *Mineralogical Magazine*, **80**, 639–646.

Pekov I.V., Zubkova N.V., Yapaskurt V.O., Polekhovsky Yu.S., Vigasina M.F., Belakovskiy D.I., Britvin S.N., Sidorov E.G. and Pushcharovsky D.Yu. (2016b) New arsenate minerals from the Arsenatnaya fumarole, Tolbachik volcano, Kamchatka, Russia. VI. Melanarsite, $K_3Cu_7Fe^{3+}O_4(AsO_4)_4$. *Mineralogical Magazine*, **80**, 855–867.

Pekov I.V., Yapaskurt V.O., Belakovskiy D.I., Vigasina M.F., Zubkova N.V. and Sidorov E.G. (2017) New arsenate minerals from the Arsenatnaya fumarole, Tolbachik volcano, Kamchatka, Russia. VII. Pharmazincite, $KZnAsO_4$. *Mineralogical Magazine*, **81**, 1001–1008.

Pekov I.V., Koshlyakova N.N., Zubkova N.V., Lykova I.S., Britvin S.N., Yapaskurt V.O., Agakhanov A.A., Shchipalkina N.V., Turchkova A.G. and Sidorov E.G. (2018a) Fumarolic arsenates – a special type of arsenic mineralization. *European Journal of Mineralogy*, **30**, 305–322.

Preprinted Article

https://doi.org/10.1180/mgm.2023.50 Published online by Cambridge University Press

Pekov I.V., Zubkova N.V., Agakhanov A.A., Yapaskurt V.O., Chukanov N.V., Belakovskiy D.I., Sidorov E.G. and Pushcharovsky D.Yu. (2018b) New arsenate minerals from the Arsenatnaya fumarole, Tolbachik volcano, Kamchatka, Russia. VIII. Arsenowagnerite, $Mg_2(AsO_4)F$. *Mineralogical Magazine*, **82**, 877–888.

Pekov I.V., Zubkova N.V., Agakhanov A.A., Belakovskiy D.I., Vigasina M.F., Yapaskurt V.O., Sidorov E.G., Britvin S.N. and Pushcharovsky D.Y. (2019a) New arsenate minerals from the Arsenatnaya fumarole, Tolbachik volcano, Kamchatka, Russia. IX. Arsenatrotitanite, $NaTiO(AsO_4)$. *Mineralogical Magazine*, **83**, 453–458.

Pekov I.V., Zubkova N.V., Agakhanov A.A., Ksenofontov D.A., Pautov L.A., Sidorov E.G., Britvin S.N., Vigasina M.F. and Pushcharovsky D.Yu. (2019b) New arsenate minerals from the Arsenatnaya fumarole, Tolbachik volcano, Kamchatka, Russia. X. Edtollite, $K_2NaCu_5Fe^{3+}O_2(AsO_4)_4$, and alumoedtollite, $K_2NaCu_5AlO_2(AsO_4)_4$. *Mineralogical Magazine*, **83**, 485–495.

Pekov I.V., Lykova I.S., Yapaskurt V.O., Belakovskiy D.I., Turchkova A.G., Britvin S.N., Sidorov E.G. and Scheidl K.S. (2019c) New arsenate minerals from the Arsenatnaya fumarole, Tolbachik volcano, Kamchatka, Russia. XI. Anatolyite, $Na_6(Ca,Na)(Mg,Fe^{3+})_3Al(AsO_4)_6$. *Mineralogical Magazine*, **83**, 633–638.

Pekov I.V., Lykova I.S., Agakhanov A.A., Belakovskiy D.I., Vigasina M.F., Britvin S.N., Turchkova A.G., Sidorov E.G. and Scheidl K.S. (2019d) New arsenate minerals from the Arsenatnaya fumarole, Tolbachik volcano, Kamchatka, Russia. XII. Zubkovaite, $Ca_3Cu_3(AsO_4)_4$. *Mineralogical Magazine*, **83**, 879–886.

Pekov I.V., Zubkova N.V., Koshlyakova N.N., Agakhanov A.A., Belakovskiy D.I., Vigasina M.F., Yapaskurt V.O., Britvin S.N., Turchkova A.G., Sidorov E.G. and Pushcharovsky D.Y. (2020a) New arsenate minerals from the Arsenatnaya fumarole, Tolbachik volcano, Kamchatka, Russia. XIII. Pansnerite, $K_3Na_3Fe^{3+}_6(AsO_4)_8$. *Mineralogical Magazine*, **84**, 143–151.

Pekov I.V., Koshlyakova N.N., Agakhanov A.A., Zubkova N.V., Belakovskiy D.I., Vigasina M.F., Turchkova A.G., Sidorov E.G. and Pushcharovsky D.Yu. (2020b) New arsenate minerals from the Arsenatnaya fumarole, Tolbachik volcano, Kamchatka, Russia. XIV. Badalovite, $NaNaMg(MgFe^{3+})(AsO_4)_3$, a member of the alluaudite group. *Mineralogical Magazine*, **84**, 616–622.

Pekov I.V., Agakhanov A.A., Zubkova N.V., Koshlyakova N.V., Shchipalkina N.V., Sandalov F.D., Yapaskurt V.O., Turchkova A.G. and Sidorov E.G. (2020c) Oxidizing-type fumaroles of the Tolbachik Volcano, a mineralogical and geochemical unique. *Russian Geology and Geophysics*, **61**, 675–688.

Preprinted Article

https://doi.org/10.1180/mgm.2023.50 Published online by Cambridge University Press

Pekov I.V., Koshlyakova N.N., Agakhanov A.A., Zubkova N.V., Belakovskiy D.I., Vigasina M.F., Turchkova A.G., Sidorov E.G. and Pushcharovsky D.Yu. (2021a) New arsenate minerals from the Arsenatnaya fumarole, Tolbachik volcano, Kamchatka, Russia. XV. Calciojohillerite, $NaCaMgMg_2(AsO_4)_3$, a member of the alluaudite group. *Mineralogical Magazine*, **85**, 215–223.

Pekov I.V., Zubkova N.V., Agakhanov A.A., Yapaskurt V.O., Belakovskiy D.I., Vigasina M.F., Britvin S.N., Turchkova A.G., Sidorov E.G. and Pushcharovsky D.Yu. (2021b) New arsenate minerals from the Arsenatnaya fumarole, Tolbachik volcano, Kamchatka, Russia. XVI. Yurgensonite, $K_2SnTiO_2(AsO_4)_2$, the first natural tin arsenate, and the katiarsite–yurgensonite isomorphous series. *Mineralogical Magazine*, **85**, 698–707.

Pekov I.V., Koshlyakova N.N., Belakovskiy D.I., Vigasina M.F., Zubkova N.V., Agakhanov A.A., Britvin S.N., Sidorov E.G. and Pushcharovsky D.Yu. (2022a) New arsenate minerals from the Arsenatnaya fumarole, Tolbachik volcano, Kamchatka, Russia. XVII. Paraberzeliite, $NaCaCaMg_2(AsO_4)_3$, an alluaudite-group member dimorphous with berzeliite. *Mineralogical Magazine*, **86**, 103–111.

Pekov I.V., Koshlyakova N.N., Belakovskiy D.I., Vigasina M.F., Zubkova N.V., Agakhanov A.A., Britvin S.N., Sidorov E.G. and Pushcharovsky D.Yu. (2022b) New arsenate minerals from the Arsenatnaya fumarole, Tolbachik volcano, Kamchatka, Russia. XVIII. Khrenovite, $Na_3Fe^{3+}_2(AsO_4)_3$, the sodium-richest alluaudite-group member. *Mineralogical Magazine*, **86**, 897–902.

Pekov I.V., Zubkova N.V., Agakhanov A.A., Yapaskurt V.O., Belakovskiy D.I., Britvin S.N., Sidorov E.G., Kutyrev A.V., Pushcharovsky D.Yu. (2023) New arsenate minerals from the Arsenatnaya fumarole, Tolbachik volcano, Kamchatka, Russia. XIX. Axelite, $Na_{14}Cu_7(AsO_4)_8F_2Cl_2$. *Mineralogical Magazine*, **87**, 109–117.

Shchipalkina N.V., Pekov I.V., Koshlyakova N.N., Britvin S.N., Zubkova N.V., Varlamov D.A. and Sidorov E.G. (2020) Unusual silicate mineralization in fumarolic sublimates of the Tolbachik volcano, Kamchatka, Russia – Part 1: Neso-, cyclo-, ino- and phyllosilicates. *European Journal of Mineralogy*, **32**, 101–119.

Petříček V., Dušek M. and Palatinus L. (2006) *Jana2006. Structure Determination Software Programs*. Institute of Physics, Praha, Czech Republic.

Sheldrick G.M. (2015) Crystal structure refinement with SHELXL. *Acta Crystallographica*, **C71**, 3–8.

Swafford S.H. and Holt E.M. (2002) New synthetic approaches to monophosphate fluoride ceramics: synthesis and structural characterization of $Na_2Mg(PO_4)F$ and $Sr_5(PO_4)_3F$. *Solid State Sciences*, **4**, 807–812.

Preprinted Article

https://doi.org/10.1180/mgm.2023.50 Published online by Cambridge University Press

Symonds R.B. and Reed M.H. (1993) Calculation of multicomponent chemical equilibria in gas-solid-liquid systems: calculation methods, thermochemical data, and applications to studies of high-temperature volcanic gases with examples from Mount St. Helens. *American Journal of Science*, **293**, 758–864.

Vergasova L.P. and Filatov S.K. (2016) A study of volcanogenic exhalation mineralization. *Journal of Volcanology and Seismology*, **10(2)**, 71–85.

Prepublished Article

https://doi.org/10.1180/mgm.2023.50 Published online by Cambridge University Press

Table 1. Chemical composition (in wt%) of evseevite.

Constituent	Holotype (#6328)			Cotype (#6260)			Probe standard
	Mean*	Range	Stand. dev.	Mean*	Range	Stand. dev.	
Na_2O	26.67	26.11 – 27.09	0.45	28.83	28.11 – 29.25	0.41	albite
K_2O	0.23	0.04 – 0.37	0.12	–	–		microcline
CaO	0.66	0.53 – 0.87	0.15	–	–		wollastonite
MgO	17.05	16.34 – 17.83	0.64	18.51	17.72 – 19.31	0.54	chromite
CuO	0.23	0.00 – 0.39	0.17	–	–		Cu
ZnO	0.30	0.21 – 0.38	0.09	–	–		ZnS
Fe_2O_3**	0.45	0.34 – 0.57	0.10	1.17	0.37 – 1.53	0.40	magnetite
SiO_2	0.22	0.16 – 0.30	0.06	–	–		wollastonite
P_2O_5	–	–		8.17	6.89 – 9.17	0.88	$LaPO_4$
As_2O_5	48.83	47.97 – 49.39	0.62	36.21	34.12 – 39.51	1.99	InAs
SO_3	–	–		2.65	0.94 – 4.53	1.55	ZnS
F	8.01	7.78 – 8.21	0.19	6.78	6.31 – 7.55	0.44	fluorophlogopite
–O=F	–3.37			–2.85			
Total	99.28			99.47			

Dash means the content below detection limit; *averaged for four spot analyses for holotype and for seven analyses for cotype; **trivalent state of admixed iron is assumed because of strongly oxidizing conditions of mineral formation in the Arsenatnaya fumarole: all iron minerals known here contain only Fe^{3+} (Pekov *et al*., 2018a).

Prepublished Article

https://doi.org/10.1180/mgm.2023.50 Published online by Cambridge University Press

Table 2. Powder X-ray diffraction data (*d* in Å) of evseevite (the holotype).

I_{obs}, %	d_{obs}	I_{calc}, %*	d_{calc}	*h k l*
14	7.05	13	7.063	020
11	6.08	10	6.087	021
2	4.982	4	4.981	110
4	4.599	3	4.600	111
100	**4.001**	100	4.007	121
5	3.831	6	3.833	112
31	**3.527**	28, 6	3.531, 3.527	040, 130
56	**3.479**	63	3.482	023
5	3.380	4	3.384	131
5	3.117	5	3.119	113
45	**3.041**	44	3.044	042
29	**2.998**	28	3.001	004
2	2.916	1	2.914	123
3	2.851	1	2.858	141
44	**2.657**	51	2.661	200
68	**2.642**	10, 64	2.646, 2.642	133, 142
36	**2.613**	40	2.614	104
6	2.494	8	2.495	150
12	2.437	7, 6	2.438, 2.433	221, 202
6	2.353	5	2.354	060
4	2.283	3	2.286	134
4	2.274	2, 2	2.275, 2.273	231, 025
1	2.187	1	2.189	213
3	2.161	2	2.161	232
2	2.128	1	2.125	240
4	2.119	2, 1	2.119, 2.117	161, 153
3	2.099	2	2.101	144
5	2.091	4	2.090	125
4	2.028	4	2.029	063
33	**2.002**	35, 4	2.003, 2.001	242, 006
16	1.992	15	1.991	204
2	1.971	2	1.972	214
3	1.918	2	1.919	154
4	1.913	4	1.912	251
6	1.895	7	1.896	163
5	1.872	4	1.873	106
3	1.856	3	1.857	116
2	1.844	2	1.843	252
1	1.833	1	1.834	234
1	1.799	1	1.800	172
15	1.765	16	1.766	080
32	**1.741**	37	1.741	046
5	1.703	4	1.703	321
2	1.690	1, 2	1.692, 1.689	262, 312
4	1.666	1, 3	1.667, 1.666	235, 027
4	1.662	3, 1	1.660, 1.660	330, 181

Pre-Published Article

https://doi.org/10.1180/mgm.2023.50 Published online by Cambridge University Press

2	1.644	3	1.645	331
5	1.613	1, 3, 3	1.615, 1.614, 1.611	083, 182, 313
4	1.602	4	1.603	165
3	1.591	1, 2	1.594, 1.590	271, 127
1	1.554	2	1.553	272
12	1.532	4, 13	1.533, 1.533	333, 342
9	1.529	6	1.527	304
5	1.524	1, 3, 1	1.525, 1.522, 1.520	066, 084, 264
3	1.502	4	1.502	350
1	1.493	1	1.491	351
6	1.471	9	1.471	280
9	1.463	12	1.463	184
11	1.457	15	1.457	246
4	1.444	6	1.444	108
1	1.433	1	1.434	217
1	1.429	1	1.429	282
4	1.412	4	1.412	227
3	1.408	1, 3	1.407, 1.407	361, 353
1	1.399	1	1.399	325

*For the calculated pattern, only reflections with intensities ≥1 are given. The strongest reflections are marked in boldtype.

Prepublished Article

https://doi.org/10.1180/mgm.2023.50 Published online by Cambridge University Press

Table 3. Comparative data of evseevite (holotype and cotype) and moraskoite.

Mineral	Evseevite (holotype)	Evseevite (cotype, P- and S-enriched variety)	Moraskoite*
Ideal formula	$Na_2Mg(AsO_4)F$		$Na_2Mg(PO_4)F$
Empirical formula	$(Na_{1.99}Ca_{0.03}K_{0.01})_{\Sigma 2.03}$ $(Mg_{0.98}Fe^{3+}_{0.01}Zn_{0.01}Cu_{0.01})_{\Sigma 1.01}$ $[(As_{0.98}Si_{0.01})_{\Sigma 1.01}O_4](F_{0.97}O_{0.03})$	$Na_{2.02}(Mg_{1.00}Fe^{3+}_{0.03})_{\Sigma 1.03}$ $[(As_{0.69}P_{0.25}S_{0.07})_{\Sigma 1.01}O_4]$ $(F_{0.78}O_{0.22})$	$Na_{1.88}(Mg_{1.06}Fe^{2+}_{0.01})_{\Sigma 1.07}$ $[P_{1.00}O_{4.00}]F_{1.00}$
Crystal system Space group	Orthorhombic *Pbcn*		Orthorhombic *Pbcn*
a, Å *b*, Å *c*, Å *V*, Å^3 *Z*	5.3224(1) 14.1255(3) 12.0047(3) 902.53(4) 8	5.307(2) 14.053(3) 11.940(3) 890.5(8) 8	5.2117(10) 13.711(3) 11.665(2) 833.6(3) 8
Strongest reflections of the powder X-ray diffraction pattern: *d*, Å – *I*, %	4.001 – 100 3.527 – 31 3.479 – 56 3.041 – 45 2.998 – 29 2.657 – 44 2.642 – 68 2.613 – 36 2.002 – 33 1.741 – 32	3.984 – 100 3.511 – 26 3.467 – 48 3.027 – 35 2.992 – 27 2.649 – 95 2.631 – 56 2.608 – 31 1.995 – 32 1.733 – 24	3.909 – 75 3.382 – 52 2.955 – 90 2.606 – 100 2.571 – 96 2.547 – 68 1.691 – 67
D_{calc}, g cm^{-3}	3.337	3.226	2.925
Optical data α β γ birefringence $2V_{meas}$	Biaxial (+) 1.545(2) 1.546(2) 1.549(2) 0.004 40(10)°	none examined	Biaxial n_{mean} = 1.550(4)** *ca.* 0.004 small
Source	this work		Karwowski *et al.*, 2015

*Powder X-ray diffraction study of moraskoite was not carried out, only the calculated data were reported.

**Probably the mean refractive index for moraskoite was determined wrongly. Our calculation of the Gladstone–Dale compatibility index for moraskoite using n_{mean} = 1.550 gave $1 - (K_p/K_c) = -0.079$, fair. Estimated value of n_{mean} for moraskoite calculated using the Gladstone–Dale equation (Mandarino, 1981) is *ca.* 1.51 [1.510 for $1 - (K_p/K_c) = 0.000$].

Prepublished Article

https://doi.org/10.1180/mgm.2023.50 Published online by Cambridge University Press

Table 4. Crystal data, data collection information and structure refinement details for evseevite (the holotype).

	Rietveld refinement	Single-crystal data
Ideal formula	$Na_2Mg(AsO_4)F$	
Formula weight	228.2	
Temperature, K	293(2)	
Radiation and wavelength, Å	Co*K*α; 1.79021	Mo*K*α; 0.71073
Crystal system, space group, *Z*	Orthorhombic, *Pbcn*, 8	
Unit cell dimensions, Å	*a* = 5.3224(1) *b* = 14.1255(3) *c* = 12.0047(3)	*a* = 5.3173(6) *b* = 14.087(2) *c* = 12.0110(13)
V, Å^3	902.53(4)	899.71(19)
Absorption coefficient μ, mm^{-1}	20.042	7.823
F_{000}	864	
Diffractometer	Rigaku R-Axis RAPID II	Xcalibur S CCD
Range for data collection, °	2θ from 9.00 to 140.00	θ from 2.892 to 28.277 -7≤ *h* ≤ 7, -4 ≤ *k* ≤ 18, 0 ≤ *l* ≤ 16
Final *R* indices	R_{exp} = 0.0069, R_{wp} = 0.0068, R_p = 0.0047, R_{obs} = 0.0435	R_1 = 0.1106, wR_2 = 0.2188 [I>2σ(I)] R_1 = 0.1376, wR_2 = 0.2314 (all data)
GoF	0.98	1.30
Largest diff. peak and hole	0.84 and -0.66 e/Å^3	2.25 and -2.25 e/Å^3
Other data		Crystal size 0.02 × 0.05 × 0.07 mm Structure solution – direct methods Refinement method – full-matrix least-squares on F^2 Absorption correction 'gaussian'

Prepublished Article

https://doi.org/10.1180/mgm.2023.50 Published online by Cambridge University Press

Table 5. Coordinates and isotropic displacement parameters (U_{iso}, in Å^2) of atoms for evseevite (the holotype).

Site	*x*	*y*	*z*	U_{iso}
As	0.70138(19)	0.88053(11)	0.58705(8)	0.0245(3)
Mg	0.7307(4)	0.51258(18)	0.8186(2)	0.0343(15)
Na(1)	0.7548(7)	0.7389(3)	0.8311(3)	0.0080(13)
Na(2)	0.7413(7)	0.6223(4)	0.5832(2)	0.0308(9)
O(1)	0.8051(9)	0.77571(18)	0.6306(4)	0.0147(6)
O(2)	0.8633(5)	0.9662(2)	0.6536(3)	0.0147(6)
O(3)	0.7442(10)	0.8930(3)	0.45019(13)	0.0147(6)
O(4)	0.3846(3)	0.8969(2)	0.6075(3)	0.0147(6)
F(1)	0.5	0.6201(3)	0.75	0.0147(6)
F(2)	0	0.5923(3)	0.75	0.0147(6)

Table 6. Selected interatomic distances (Å) in the structure of evseevite (the holotype).

As – O(1)	1.665(3)	Na(1) – O(1)	2.477(6)
- O(2)	1.687(3)	- O(1)	2.443(6)
- O(3)	1.668(2)	- O(3)	2.349(5)
- O(4)	1.7194(19)	- O(4)	2.465(5)
As – O	**< 1.685 >**	- F(1)	2.367(5)
		- F(2)	2.634(5)
Mg – O(2)	2.089(4)	**Na1 – (O,F)**	**< 2.456 >**
- O(2)	2.145(4)		
- O(3)	2.071(4)	Na(2) – O(1)	2.266(6)
- O(4)	2.031(4)	- O(2)	2.426(6)
- F(1)	2.120(4)	- O(3)	2.685(7)
- F(2)	2.000(3)	- O(3)	2.715(7)
Mg – (O,F)	**< 2.076 >**	- O(4)	2.429(5)
		- F(1)	2.379(3)
		- F(2)	2.467(3)
		Na2 – (O,F)	**< 2.894 >**

Table 7. Bond valence calculations for evseevite (the holotype).

	As	Mg	Na(1)	Na(2)	Σ
O(1)	1.33		0.16 0.17	0.26	1.92
O(2)	1.25	0.34 0.30		0.18	2.07
O(3)	1.32	0.35	0.21	0.09 0.09	2.06
O(4)	1.14	0.38	0.16	0.17	1.85
F(1)		$0.23^{x2\rightarrow}$	$0.15^{x2\rightarrow}$	$0.15^{x2\rightarrow}$	1.06
F(2)		$0.32^{x2\rightarrow}$	$0.08^{x2\rightarrow}$	$0.12^{x2\rightarrow}$	1.04
Σ	5.04	1.92	0.93	1.06	

Bond-valence parameters for As-O, Mg-O and Na-O are taken from Gagné & Hawthorne (2015), and for Mg-F and Na-F from Brese & O'Keeffe (1991).

Prepublished Article

https://doi.org/10.1180/mgm.2023.50 Published online by Cambridge University Press

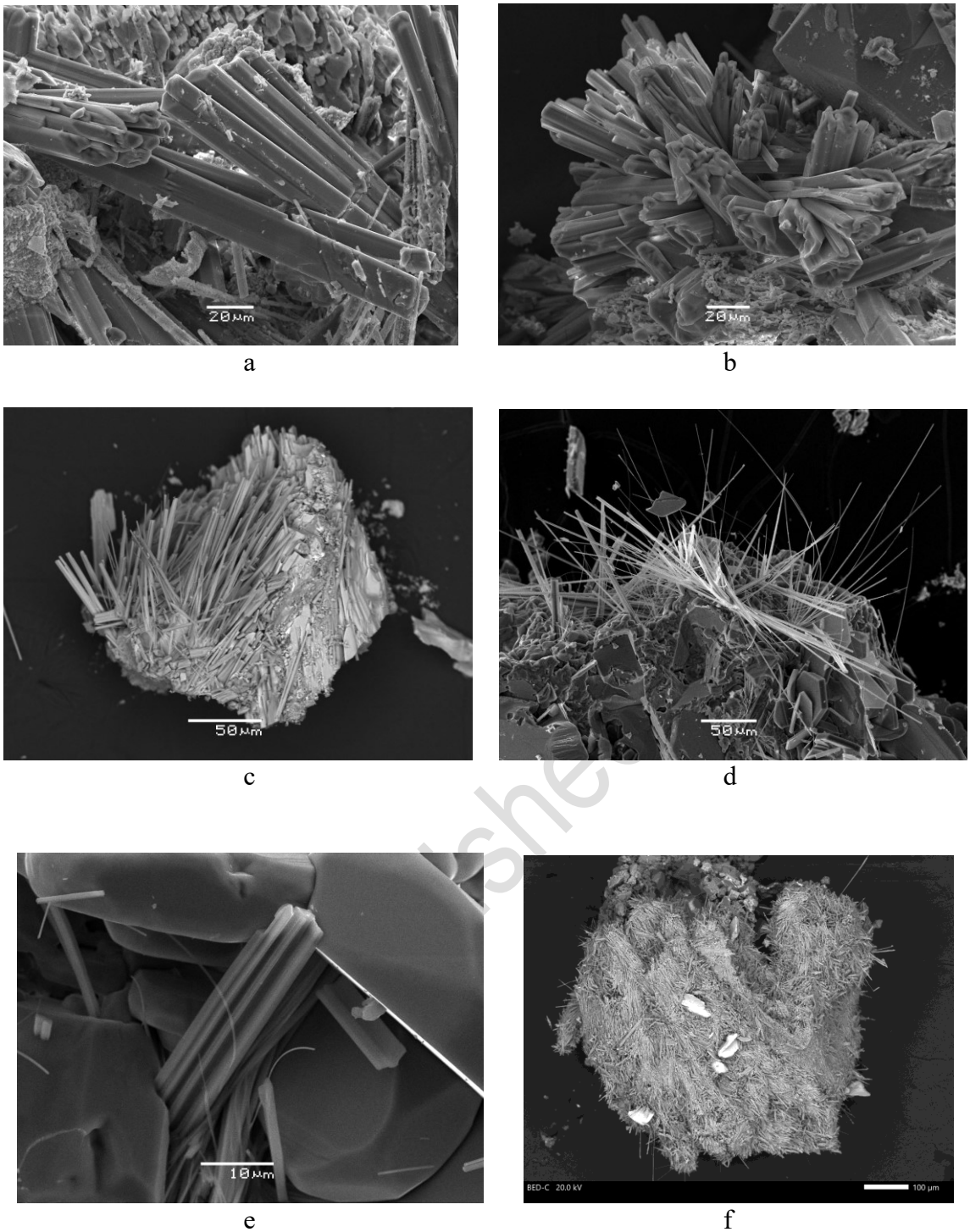

a b c d e f

Fig. 1. Morphology of evseevite: (*a–c*: holotype, #6328) – aggregates of prismatic to acicular crystals overgrowing badalovite (*b* – with large hematite crystal); (*d–e*: cotype, #6260) – long-prismatic to acicular and hair-like crystals on hematite and fluorophlogopite; *f* – sample #7529, pilous crust completely covering calciojohillerite crystals (with bright white tenorite crystals). SEM images, SE (*a*, *b*, *d*, *e*) and BSE (*c*, *f*) modes.

https://doi.org/10.1180/mgm.2023.50 Published online by Cambridge University Press

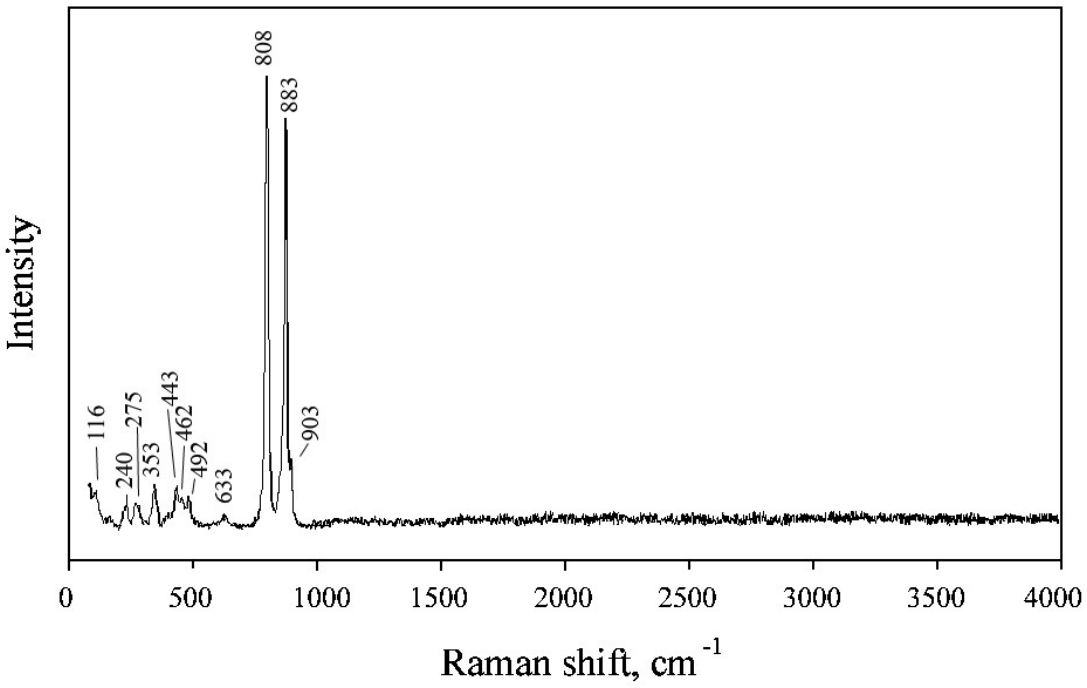

Fig. 2. The Raman spectrum of evseevite (the holotype).

Prepublished A

https://doi.org/10.1180/mgm.2023.50 Published online by Cambridge University Press

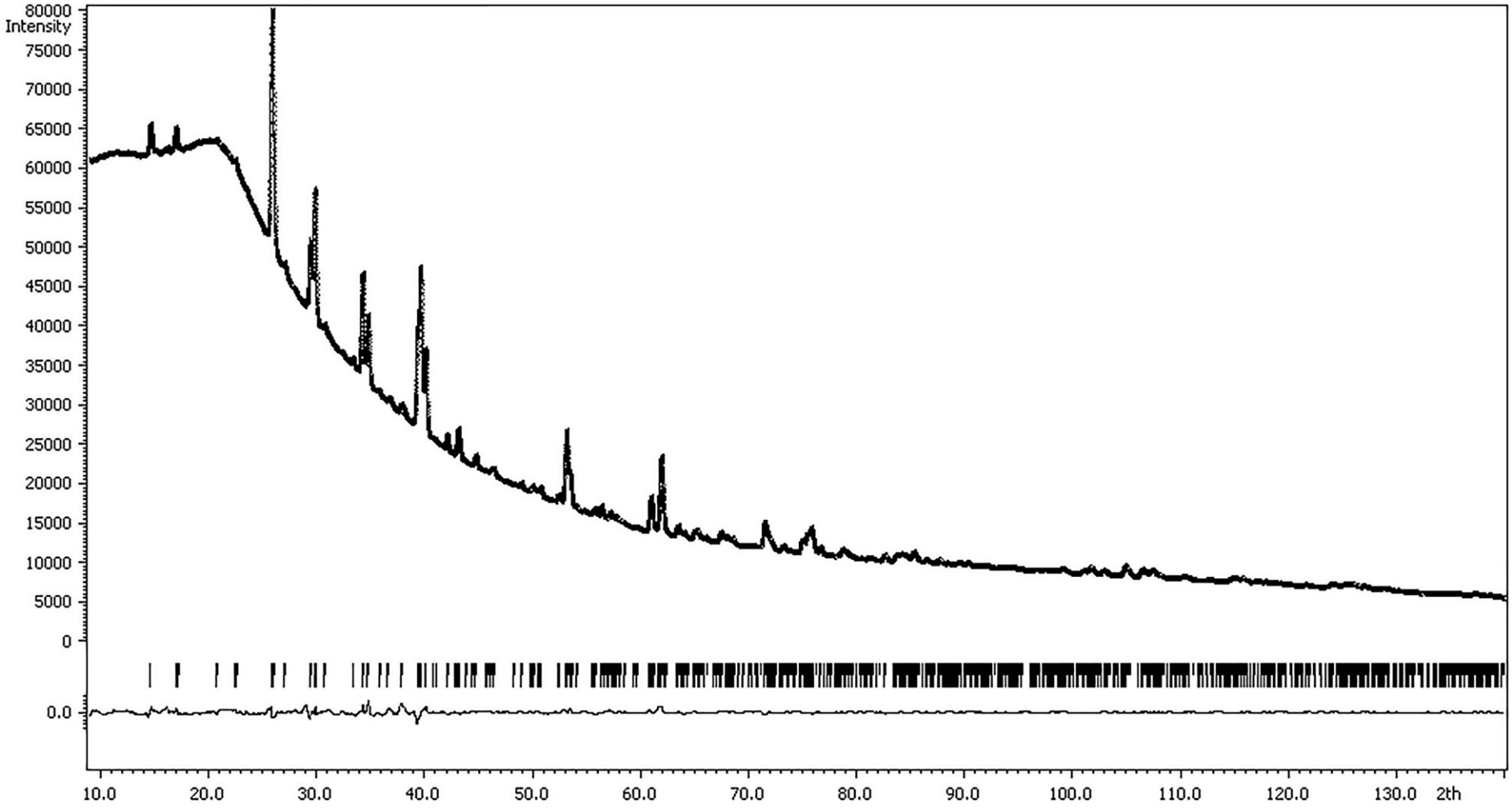

https://doi.org/10.1180/mgm.2023.50 Published online by Cambridge University Press

Fig. 3. Measured and calculated powder X-ray diffraction patterns of evseevite (the holotype). The solid line corresponds to calculated data, the crosses correspond to the measured pattern, vertical bars mark all possible Bragg reflections. The difference between the measured and calculated patterns is shown by curve at the bottom.

Prepublished Article

https://doi.org/10.1180/mgm.2023.50 Published online by Cambridge University Press

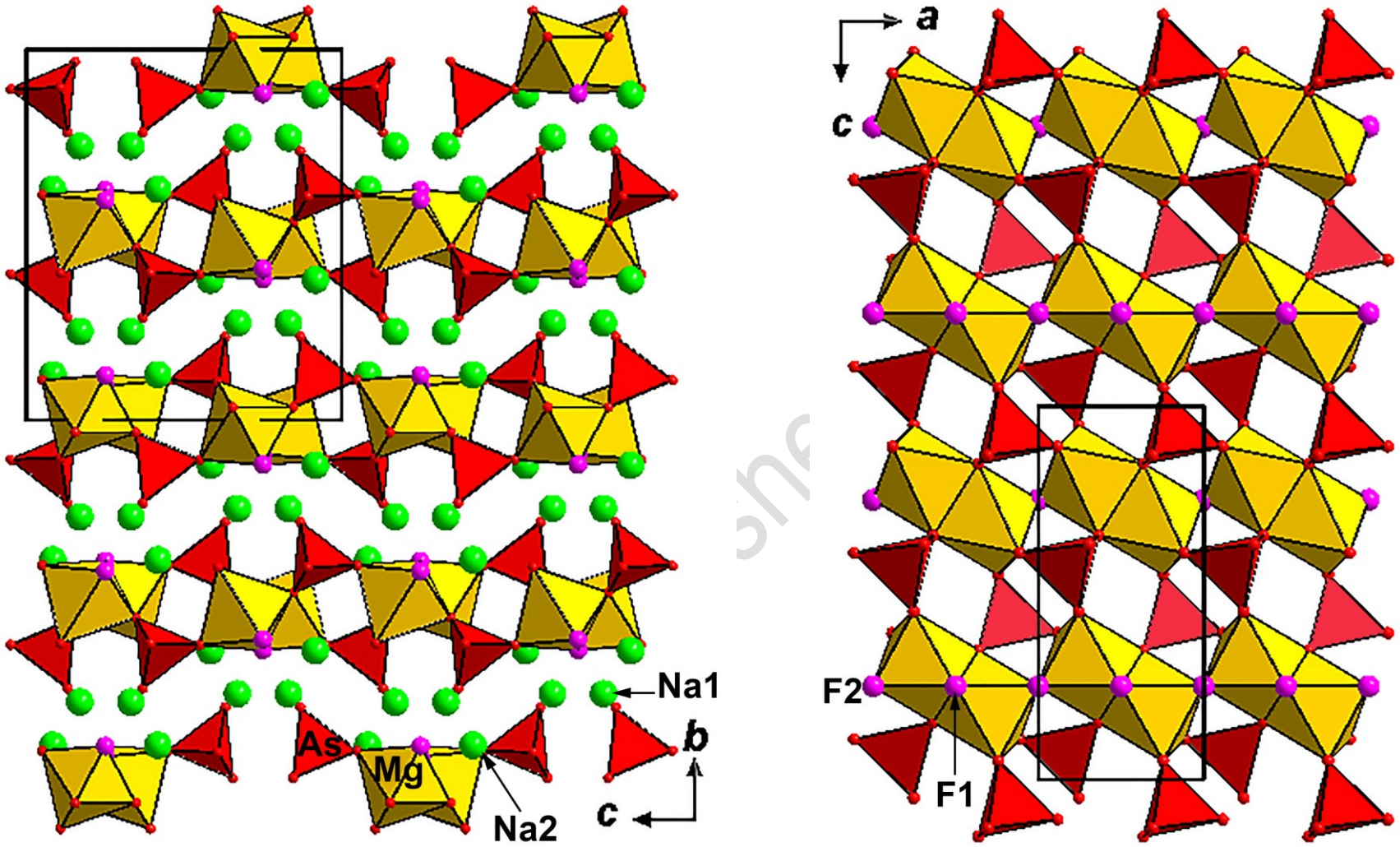

a) b)

Fig. 4. The crystal structure of evseevite projected along the *a* axis (a) and heteropolyhedral layer in it (b). The unit cell is outlined.

https://doi.org/10.1180/mgm.2023.50 Published online by Cambridge University Press

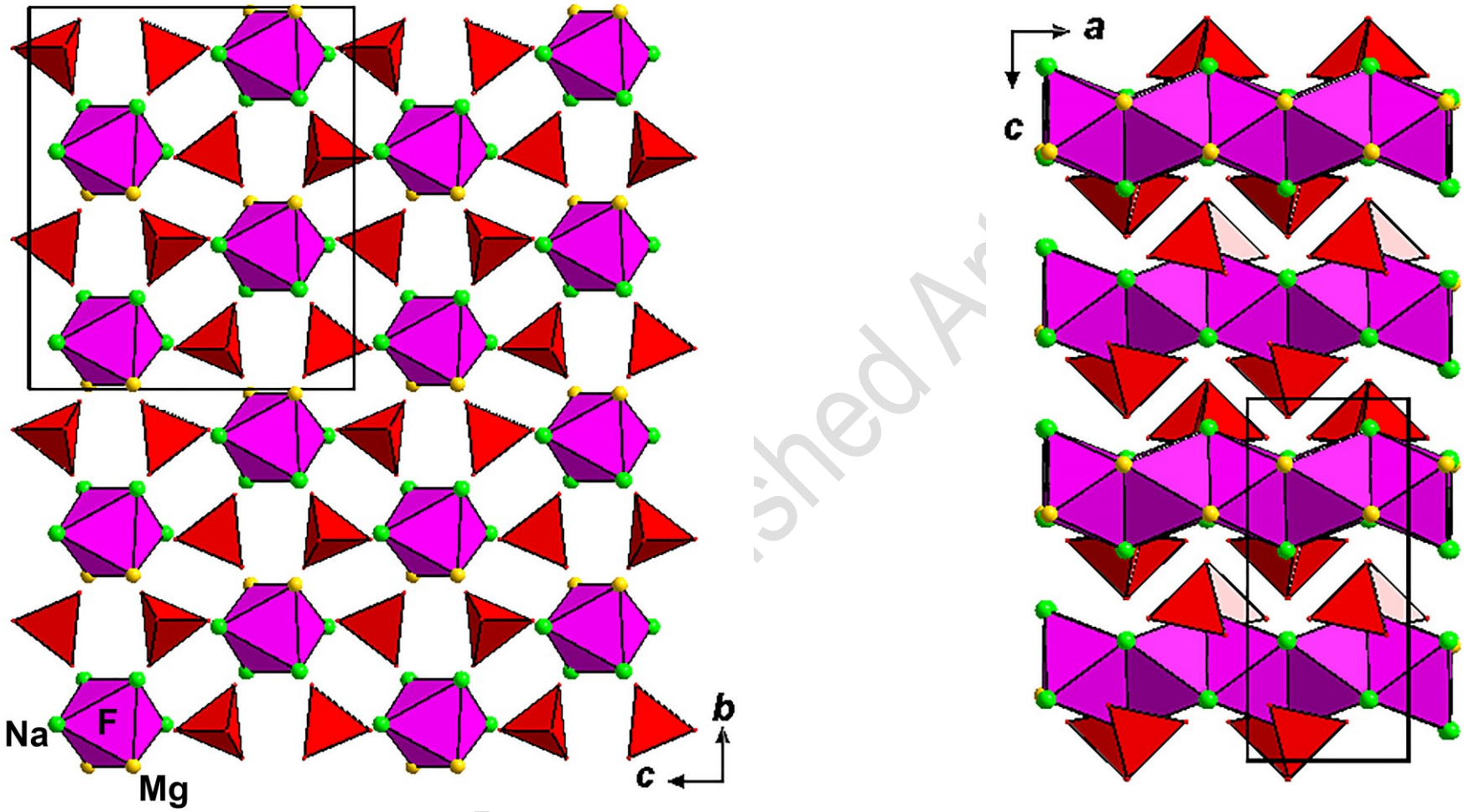

a) b)

Fig. 5. F-centred octahedra FNa_4Mg_2 and AsO_4 tetrahedra in the structure of evseevite (two projections). The unit cell is outlined.

https://doi.org/10.1180/mgm.2023.50 Published online by Cambridge University Press